VIII International Conference on Fracture Mechanics of Concrete and Concrete Structures
FraMCoS-8
J.G.M. Van Mier, G. Ruiz, C. Andrade, R.C. Yu and X.X. Zhang (Eds)

MODELLING CRACKING AND BENDING FAILURE OF SFRC BEAMS WITH CONVENTIONAL REINFORCEMENT

DAVID FALL*†, RASMUS REMPLING†, ANETTE JANSSON† AND KARIN LUNDGREN†

†Chalmers University of Technology
Civil and Environmental Engineering, Sven Hultins Gata 8, 412 96 Gteborg, Sweden
e-mail: david.fall@chalmers.se, www.chalmers.se

Key words: Steel fibre reinforced concrete, Reinforced concrete beams, Non-linear FE-modelling, Fib Model Code 2010

Abstract. In this study three beams, with varying contents of steel fibre reinforcement, were tested in four point bending and compared with results from FE-analysis. The beams were part of a larger experimental programme where relevant material properties were investigated.

FE-modelling was performed using a two dimensional model. Concrete was represented by four-node quadrilateral isoperimetric plane stress elements. The smeared crack approach was utilized and the stress-strain relation describing the tensile behavior of the concrete was calculated from uni-axial test results, assuming the crack bandwidth to be equal to the element length. In compression, the concrete was assumed to behave elasto ideal-plastic. The reinforcement was modelled by straight 2-node truss elements connected to the concrete by two-dimensional interface elements providing the bond-slip properties. A material model including hardening effects was derived from tension tests of reinforcement bars and used for modelling the conventional reinforcement. A multi-linear bond-slip model was established through pull-out tests. As an alternative, analyses were also performed taking into account a reduction of the bond stress after yielding of the reinforcement occurred. Loading was applied in two phases: the first comprehending only the self-weight, while incremental loading was applied by deformation control during the second phase.

General agreement between experiments and FE-analyses was obtained with regard to load-displacement behaviour. By observing the crack patterns, both from FE-analysis and experiments, it can be concluded that the general behaviour agreed; however, in the analyses not all cracks were fully localized. A higher degree of crack localization was obtained when the bond loss at yielding was included.

1 INTRODUCTION

The use of steel fibre reinforcement (SFRC) has increased during the last two decades. However, there is a lack of experiments in the scale of structural elements, in which the material properties are well-defined enough to facilitate model validation. Several researchers have studied laboratory scale tests with the purpose to determine material properties for SFRC. Approaches of determining the tensile behaviour of SFRC have been discussed in numerous articles. In RILEM TC 162-TDF [1] and RILEM TC 162-TDF [2], methods based on uniaxial testing and beam bending, respectively, were suggested. Such approaches have been studied by e.g. Kooiman et al. [3] and Giaccio et al. [4]. In addition to these methods, a wedge-splitting procedure was proposed [5]. Larger scale beams have been studied by several researchers [6, 7, 8, 9]. The current study was

performed in order to evaluate the recently published International Federation for Structural Concrete (fib) [10] (MC 2010) and to contribute to the field of SFRC-modelling. Establishing a broad knowledge of the structural behavior and modelling approaches of SFRC is important in order to enable a wider usage of the technology. By combining well-defined experimental work, non-linear finite element analysis and results obtained in accordance with MC 2010, this paper ultimately evaluates the structural engineering approaches to SFRC.

2 EXPERIMENTAL PROGRAMME

The experimental programme comprised uniaxial testing, pull-out tests, reinforcement tension tests and four-point bending test of reinforced beams. This paper focuses on the concrete beams; however, the other experiments are also described here in concentrated form as they are significant while discussing the validity of the model, presented in Section 3. Full descriptions of the pull-out tests and unaxial tests are provided in Jansson et al. [11] and Jansson et al. [12], respectively.

2.1 Four-point bending

Three SFRC beams of fibre content 0.0, 0.25 and 0.5% (percent by volume) were tested in deformation controlled four-point bending. The beams were simply supported and spanned 1800 mm, with shear spans of 600 mm, see Figure 1. Each beam was reinforced with three reinforcement bars: $\phi 8$ in the beams of fibre content 0.0 and 0.5% and $\phi 6$ in the beam of fibre content 0.25%. Steel quality was B500BT (Swedish quality). Shear reinforcement (stirrups) was included over the supports. Fibre content, reinforcement configurations and tested concrete strengths for all beams are presented in Table 1.

2.2 Material

The concrete used for all the experiments was self-compacting and mixed in a central drum-mixer at a ready-mix plant, in batches of 2 m^3 [11]. The fibres used were end-hooked steel fibres, Dramix®RC 65/35-BN from Bekaert, with a tensile strength of 1100 MPa, and the actual fibre content was estimated performing washout control in accordance with governing standard [13]. The compressive strength ($f_{ccm.28d}$), elastic modulus (E_{cm}) and splitting tensile strength ($f_{ctm.28d}$) was determined according to european standards [14, 15, 16]. To capture the softening behaviour of the fibre reinforced concrete ($\sigma - w$ relation), uni-axial tensile testing was performed on notched cylinders, in accordance with RILEM TC 162-TDF [1]. The tests were performed in accordance with RILEM TC 162-TDF [1] at the Technical Research Institute of Sweden and are further described in Jansson et al. [12]. In Figure 2 the test setup is presented.

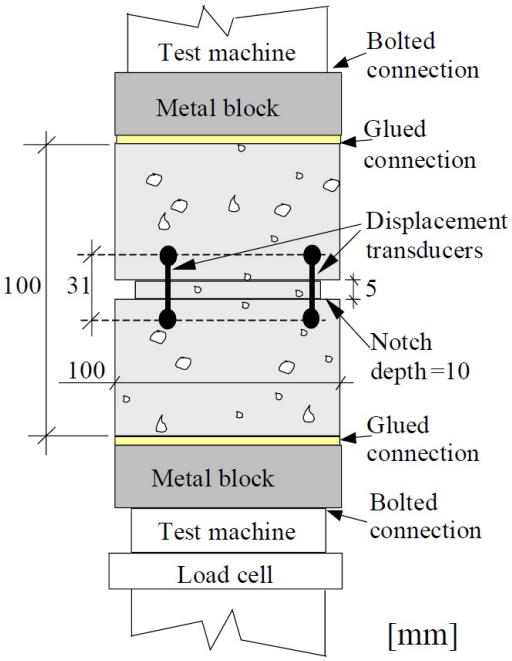

Figure 2: Geometry and test setup for uni-axial testing, Jansson et al. [12].

Tension tests were performed to determine the behaviour of the reinforcement bars. Each series ($\phi 6$ and $\phi 8$) included 5 bars. In addition to this the bond properties between reinforcement bars and concrete were determined by pull-out tests, see Figure 3. To avoid wall effects the tested specimens were cut out from larger prisms of 110x152x720 mm^3; the spec-

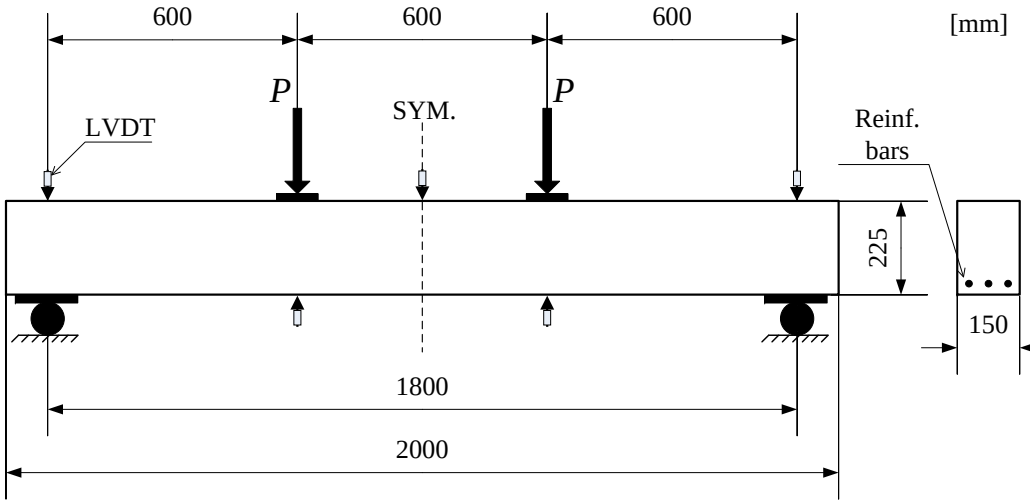

Figure 1: Experimental set-up

Table 1: Test beam configurations

Beam No.	I	II	III
V_f, nominal	0.00%	0.25%	0.50%
V_f, actual (mean value from wash-out)	0.00%	0.18%	0.45%
Reinforcement	3ϕ8	3ϕ6	3ϕ8
$f_{ccm.28d}$	58.8 MPa	58.1 MPa	57.5 MPa
$f_{ctm.28d}$	2.9 MPa	2.7 MPa	3.0-3.1 MPa
E_{cm}	32.5 GPa	30.5 GPa	31.0 GPa

imen dimensions were 112x112x110 mm^3. A ribbed ϕ16 bar of quality B500BT was placed in the square cross-section centre. Specimen size was chosen so that the concrete surface strains would be measurable while delaying splitting in the series without steel fibre reinforcement as long as possible. Five specimens were tested for each fibre content. Full description of experiments and results is given in Jansson et al. [11].

Results from the described uni-axial, tension and pull-out tests are presented as model input data in Section 3.2.

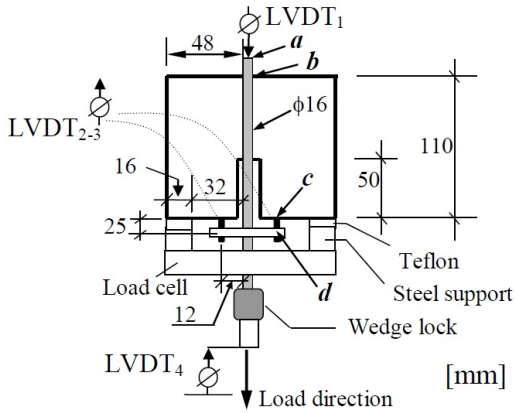

Figure 3: Geometry and test setup for pull-out testing, Jansson et al. [11].

3 NON-LINEAR FINITE ELEMENT ANALYSIS

Non-linear finite element analyses were performed using the commercial FE-software TNO DIANA [17]. A phased loading procedure was used. In the first of two loading phases, the selfweight was applied and incremental loading was applied by deformation control during the second phase. The model geometry and the material models used are described in the following two sections, respectively.

3.1 Geometry

A dense quadratic mesh (5x5 mm) of four-node quadrilateral isoperimetric plane stress elements was used for concrete representation. The reinforcement bars were modeled by straight 2-point truss elements connected to two-dimensional interface elements to which the bond-slip properties were assigned. As a measure for rationalising the computations, only half beam was modelled due to symmetry, see Figure 4. In the symmetry line, all movement in the horizontal direction was constrained. Support and loading plates were modeled using eccentric tyings, i.e. the vertical movement of the nodes at the plates was maintained on a straight line intersecting the plate center node. Regions acting under these assumptions were 150 and 100 mm wide for the support node and the loading node, respectively. The centre node in the support was constrained from vertical movement.

3.2 Material models

Nonlinear fracture mechanics with rotating cracks were used for concrete modeling. As previously mentioned, the tensile properties of the concrete were determined by uniaxial tension tests. A smeared crack approach was utilised. The stress-strain relation used for concrete in tension was calculated from the crack-widths measured in these tests, w_i, in accordance with Equation 1. The crack bandwidth, h, was assumed to be equal to the element length. The stress-crackwidth relation can be seen in Figure 5.

$$\varepsilon_i = \frac{f_\mathrm{t}}{E} + \frac{w_i}{h}. \tag{1}$$

For compression, an elasto ideal-plastic compressive behavior was used. In addition to this relatively simple material model a built-in DIANA function [17], based on the theory of Vecchio and Collins [18], was applied. In short this function reduces the compressive stresses in elements with large tensile stresses perpendicular to the principal compression direction. Furthermore, the elastic modulus was assumed to be linear during the uncracked state and was established from the uniaxial tension tests, see Table 1.

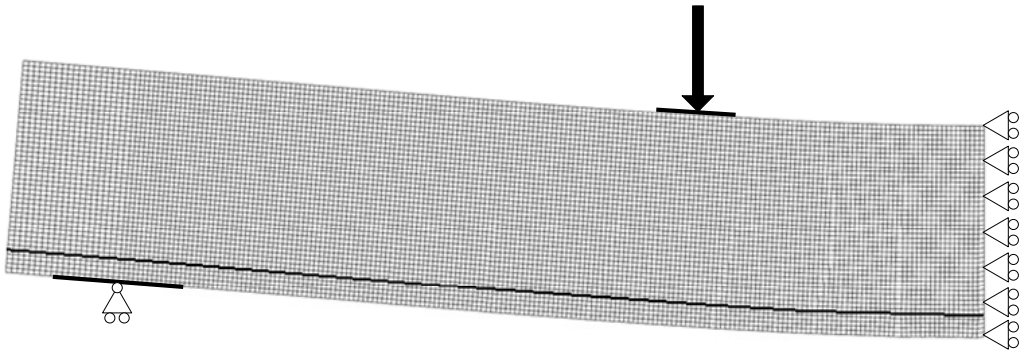

Figure 4: Model geometry. Eccentric boundary conditions (tyings) and the reinforcement position are indicated with thick black lines.

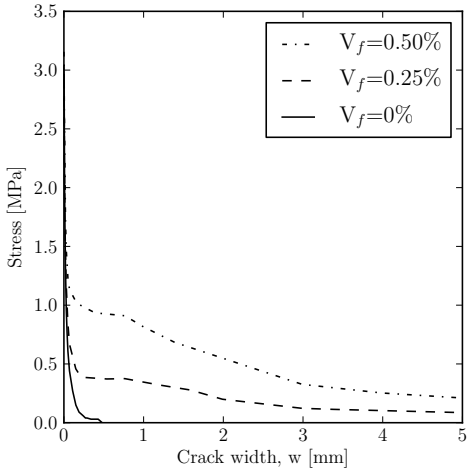

(a)

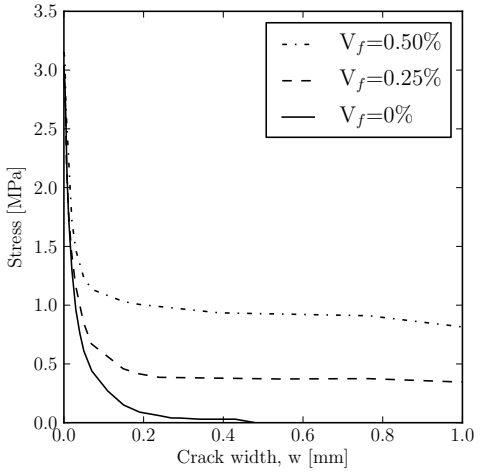

(b)

Figure 5: (a) Input used for concrete tensile behavior. (b) Detail for crack widths up to 1 mm.

A material model that included hardening effects was used for conventional reinforcement bars. In the model, the average nominal diameter of the tested reinforcement bars was used. The corresponding input is shown in Figure 6.

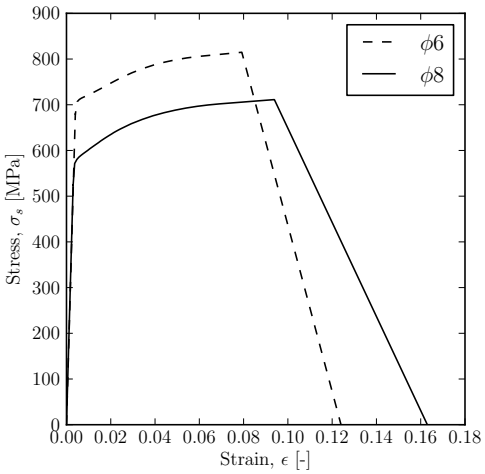

Figure 6: Input for the reinforcement bars.

As decribed in Section 2.2, the bond-slip behavior was measured in the pull-out tests. Noteworthy is that the pull-out tests were performed on specimens with reinforcement bar diameter of 16 mm. However, as the ratio between the concrete cover thickness and the bar diameters is approximately the same in the pull-out specimens and beams, the bond stress versus slip

measured in the pull-out tests was assumed to be directly applicable as input in the modeling of the beams.

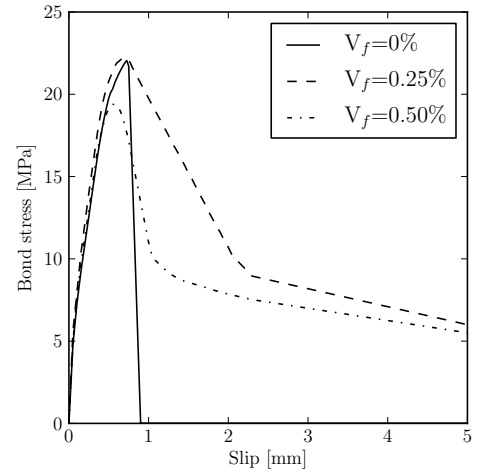

(a)

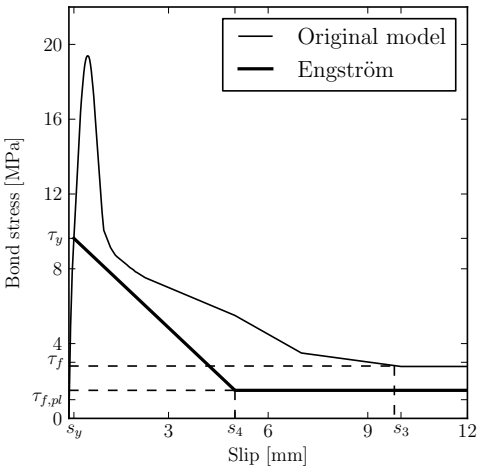

(b)

Figure 7: (a) Experimentally obtained bond stress versus slip used as input. (b) Bond stress versus slip, original model and modification when yielding occurs in reinforcement (V_f=0.50%).

Several researchers have observed that the bond stress is reduced after reinforcement yielding [19, 20]. To study the effect of of this phenomenon on the model behaviour analyses were carried out on two types of models: one in which the bond stress depended only on the slip, and one in which the bond stress was reduced one the reinforcement reached yielding stress. In the latter case, the model of Engström [20] was applied, reducing the bond stress linearly towards the suggested values $\tau_{f,pl} = 0.5\tau_f$ and $s_4 = 0.5s_3$, see Figure 7. It should be pointed out that contrary to what would be expected, the average bond capacity of the pull-out tests with $V_f = 0.50\%$ was lower than the average of the ones with less fibre content ($V_f = 0.25\%$). This is due to large scatter in the experimental results of the fibre content $V_f = 0.50\%$. In pull-out tests with higher fibre content ($V_f = 1.0\%$), presented in Jansson et al. [11], both the maximum and residual bond capacity increased.

4 RESULTS

The focus of this section is on the comparison between the performed beam tests and the FE-analyses. First load-deflection curves and crack patterns are presented and in Section 4.1 the effect of bond reduction at yielding are discussed. Noteworthy is that also the results from calculations according to MC 2010 are presented. Detailed information on these calculations are presented in Fall et al. [21].

Comparing the load-deflection curves in Figure 8, a general agreement can be seen between the experimental results and the results obtained trough FE analysis. For all beams a stiffness loss can be observed as the first crack develops. Thereafter, the stiffness is relatively constant until the reinforcement yields. All three beams failed in bending. Furthermore, it can be seen that the calculations in accordance with MC 2010 gives results well on the safe side, both in terms of ultimate load and deflection. For the particular structural member analysed in this study the magnitude of the underestimation increases with increasing fibre content. The FE analysis were generally stable and usually converged until some load steps after yielding occurred in the reinforcement. For larger deflections, the analyses did not converge in all steps; hence the small disturbances, which can be seen in Figure 8.

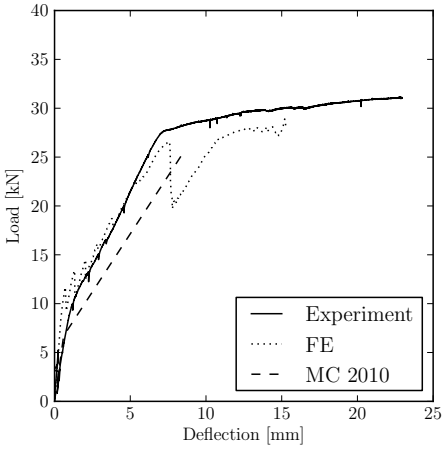

(a) V_f=0.00%, 3ϕ8

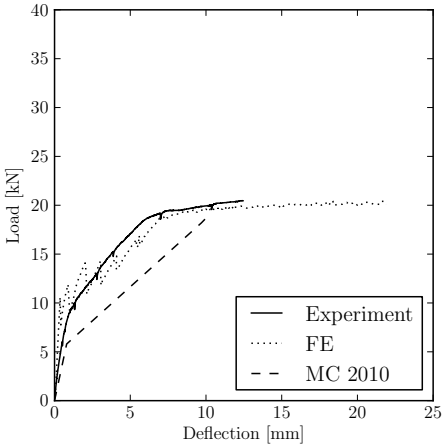

(b) V_f=0.25%, 3ϕ6

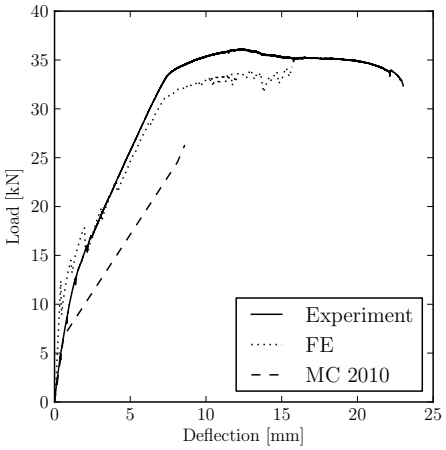

(c) V_f=0.50%, 3ϕ8

Figure 8: Load deflection behaviour (mid span): results from experiments, MC 2010 analysis and FE-modeling with improved bond model [20]

Considering the FE analysis of the beam without fibres, a sudden loss of stiffness was observed just after the yielding of the reinforcement (at a load of approximately 27kN), see Figure 8. It was observed that tensile strains developed locally in the elements surrounding the reinforcement bar, as a continuation of an inclined crack. The main direction of these cracks were along the bars; thus the crack pattern was similar to shear-splitting failure after this point.

In addition to the general agreement previously discussed, also the number of cracks, total spread of cracks and the distance between them agreed roughly comparing the experiments and results from the FE-analysis. Some of the differing results can be explained by imperfections in the test samples and set-up. A comparison of modelled crack pattern and the one obtain in experiment can be found in Fall et al. [21]. Some examples of modelled crack patterns are shown in Figure 9.

4.1 Influence of bond reduction at yielding

As previously described in Section 3.2, two analyses of each beam were carried out: one with original bond-slip model and one where the bond stress was linearly decreased with increased slip once yielding occurred in the reinforcement bar [20]. There was no difference in cracking before yielding of the reinforcement, as the two bond models were completely equivalent up until this point, see Figure 9. As expected the cracks were more clearly localized when the bond stress is reduced at yielding. This is due to the fact that when the bond stress does not increase after yielding of the reinforcement, no new cracks form.

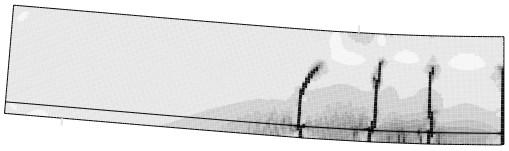

(a) V_f=0.50%, prior yielding with original bond model

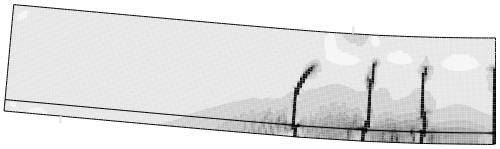

(b) V_f=0.50%, prior yielding with bond model according to Engström [20]

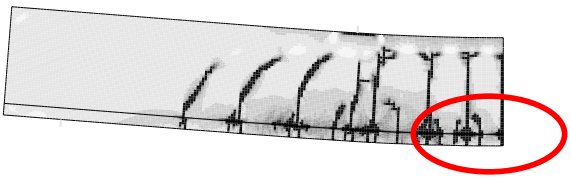

(c) V_f=0.50%, after yielding with original bond model

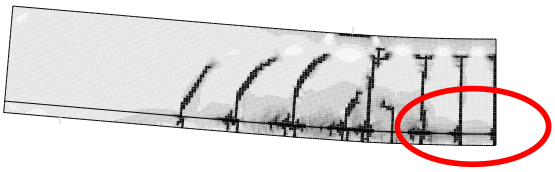

(d) V_f=0.50%, after yielding with bond model according to Engström [20]

Figure 9: Examples of crack patterns (V_f=0.50%) corresponding to the applied deformation 2.7 mm (a, b) and 14 mm (c, d). The difference in crack localization after yielding of the reinforcement occurred is indicated.

4.2 Modelling of beams with equal conventional reinforcement

In order to increase the comparability of the various beam configurations a modelling seria was made in which the same dimension of reinforcement bar was assumed. As expected the behaviour were approximately equal for all beams in the elastic phase. In the phase with cracking and, eventually, yielding of the reinforcement the fracture energy was much higher in the fibre reinforced beams. The results from this study, in terms of load deflection behaviour, can be seen in Figure 10.

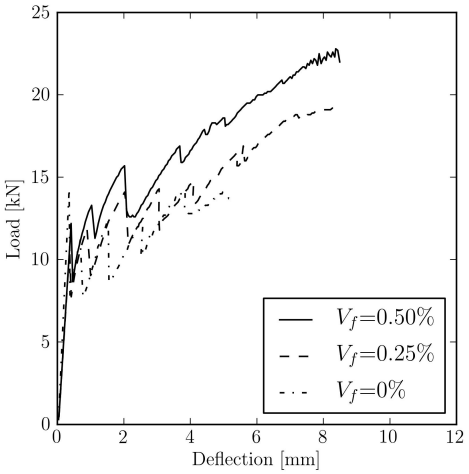

Figure 10: Modelled load deflection behaviour (mid span) for beams reinforced with equal configurations of conventional reinforcement ($3\phi6$).

5 CONCLUSIONS

To conclude, it can be seen that the increased post cracking capacity of SFRC, seen in experiments, can be estimated with FE-analysis. Furthermore, reasonable agreement was also obtained with regards to crack patterns when comparing experiments and FE-analyses. Utilizing a bond-stress model where the bond stress is reduced post yielding, resulted in more localized crack patterns. Modeling fibre reinforced concrete with non-linear finite element method, utilizing a 2D-model with plane stress elements were shown to be successful provided that material data is chosen with care. In addition to the study in which experiment and modelling was compared, models were also established with equal amount of conventional reinforcement, but varying content of steel fibre reinforcement. As expected the post cracking capacity became higher with increasing amount of fibres.

However, in the studied beams, Model Code 2010 (MC 2010) fails to fully quantify the post

cracking capacity added by the steel fibre reinforcement. The method proposed in MC2010 underestimates the additional capacity provided by the addition of steel fibres, both with regards to load and deformation capacities. The underestimation increases with increased fibre content.

6 ACKNOWLEDGEMENT

The presented experiments were financed by Thomas Concrete Group AB. All other parts of this research were funded from the European Community's Seventh Framework Programme under grant agreement NMP2-LA-2009-228663 (TailorCrete). More information on the research project TailorCrete can be found at www.tailorcrete.com.

References

[1] RILEM TC 162-TDF, 2001. Uni-axial tension test for steel fibre reinforced concrete. *Mater. and Struct.* **34**(1):3–6.

[2] RILEM TC 162-TDF, 2002. Bending test. *Mater. and Struct.* **35**(9):579–582.

[3] Kooiman, A. G., Van Der Veen, C. and Walraven, J. C., 2000. Modelling the post-cracking behaviour of steel fibre reinforced concrete for structural design purposes. *Heron.* **45**(4):275–307.

[4] Giaccio, G., Tobes, J. and Zerbino, R., 2008. Use of small beams to obtain design parameters of fibre reinforced concrete. *Cem. and Concr. Compos.* **30**(4):297 – 306.

[5] Löfgren, I., Stang, H. and Olesen, J., 2005. Fracture properties of frc determined through inverse analysis of wedge splitting and three-point bending tests. *J. of Adv. Concr. Technol.* **3**(3):423–434.

[6] Noghabai, K., 2000. Beams of fibrous concrete in shear and bending: Experiment and model. *ASCE J. of Struct. Eng.* **126**(2):243–251.

[7] Jansson, A., Löfgren, I. and Gylltoft, K., 2010. Flexural behaviour of members with a combination of steel fibres and conventional reinforcement. *Nordic Concr. Res.* (42):155–171.

[8] Özcan, D., Bayraktar, A., Sahin, A., Haktanir, T. and Türker, T., 2009. Experimental and finite element analysis on the steel fiber-reinforced concrete (sfrc) beams ultimate behavior. *Constr. and Building Mater.* **23**(2):1064–1077.

[9] Altun, F., Haktanir, T. and Ari, K., 2007. Effects of steel fiber addition on mechanical properties of concrete and rc beams. *Constr. and Building Mater.* **21**(3):654 – 661.

[10] International Federation for Structural Concrete (fib), 2010. *Bulletin 55-56: Model Code 2010 First Complete Draft*. CEB/FIP.

[11] Jansson, A., Löfgren, I., Lundgren, K. and Gylltoft, K., 2012. Bond of reinforcement in self-compacting steel-fibre reinforced concrete. *Mag. of Concr. Res.* **64**(7):617–630.

[12] Jansson, A., Flansbjer, M., Löfgren, I., Lundgren, K. and Gylltoft, K., 2012. Experimental investigation of surface crack initiation, propagation and tension stiffening in self-compacting steel-fibre reinforced concrete. *Mater. and Struct.* **45**(8):1127–1143.

[13] SIS, 2005, SS-EN 14721:2005 Test method for metallic fibre concrete - Measuring the fibre content in fresh and hardened concrete. Swedish Standards Institute (SIS).

[14] SIS, 2009, SS-EN 12390-3:2009 Testing hardened concrete - Part 3: Compressive strength of test specimens. Swedish Standards Institute (SIS).

[15] SIS, 2005, SS-EN 137232:2005 Concrete testing - Hardened concrete - Modulus of elasticity in compression. Swedish Standards Institute (SIS).

[16] SIS, 2009, SS-EN 12390-6:2009 Testing hardened concrete - Part 6: Tensile splitting strength of test specimens. Swedish Standards Institute (SIS).

[17] TNO DIANA, 2010. *Finite element analysis, Users Manual Release 9.4.3*. TNO Diana, Delft.

[18] Vecchio, F. J. and Collins, M. P., 1993. Compression response of cracked reinforced concrete. *J. of Struct. Eng.* **119**(12):3590–3610.

[19] Shima, H., Chou, L. and Okamura, H., 1987. Bond Characteristics in Post-Yield Range of Deformed Bars. *Concr. Libr. Int.* (10):113–124.

[20] Engström, B., 1992. *Ductility of Tie Connections in Precast Structures*. Dissertation, Chalmers University of Technology, Gothenburg.

[21] Fall, D., Rempling, R., Jansson, A., Lundgren, K. and Gylltoft, K., 2012. Steel fibres in reinforced beams: Experiments, model code and FE-analyses. *Submitted to Mater. and Struct* .